

On a Robust, Sensitive Cell – Free Method for Pseudomonas Sensing and Quantification

Jong Seto^{1*}, P.J. Buske^{1,2,#}, Matthew Laurie³

¹Department of Bioengineering and Therapeutic Sciences, University of California at San Francisco and California Institute for Quantitative Biosciences (QB3), 1700 4th Street, Byers Hall #303, San Francisco, CA 94158

²Department of Cell and Molecular Pharmacology, University of California at San Francisco and California Institute for Quantitative Biosciences (QB3), 600 16th Street, Genentech Hall #N314, San Francisco, CA 94143

³Department of Biochemistry and Biophysics and Tetrad Graduate Program, University of California at San Francisco and California Institute for Quantitative Biosciences (QB3), 1700 4th Street, Byers Hall #403, San Francisco, CA 94158

#Presently at: MedImmune, LLC, 319 Bernardo Avenue, Mountain View, CA 94043

*Corresponding author: jong.seto@ucsf.edu

Cell – free lysates have found a utility in performing cellular functions and providing biologically-relevant metabolic products without the optimal biological conditions for growth and proliferation. By teasing out the biological components and constructing artificial conditions that enable for biological transcription and translation processes to occur, specific cell - like functions can be reconstituted *in vitro* without requiring the entire cell and *milieu* of cellular organelles. This enables for optimization of biological circuits, either by concentration or on/off switches, simply through the addition or removal of genetic components (plasmids, inducers, or repressors) of regulatory elements. Here, we demonstrate an application of cell – free process that is robust and portable, independent of a substrate, to apply for sensing and reporting functions of a quorum sensing molecule N-3-oxododecanoyl homoserine lactone (3OC12HSL) found crucial for pathological Pseudomonas infections. Using droplet microfluidics to integrate cell – free related functions into hydrogel scaffolds, we show that these cell - free circuits can be encapsulated, delivered, and activated in most environments—even in conditions with very little hydration.

Introduction

Biological engineering of organisms and natural systems have ushered novel methods to examine disease and dysfunction *in vivo* [1-5]. Recent innovations using cell – free lysates for various functions have led to a variety of applications from biocomputation [6, 7] molecular design and engineering [8, 9], metabolic pathway engineering [10-12] to novel methods of protein synthesis [13-15]. In all these examples of cell – free lysate applications, the underlying premise of transcription and translation is still relied upon [16, 17]; however, with modifications and the addition of synthetic energy pathways, these cellular processes can be engineered to operate *ex vivo*.

A range of cell types have been explored for cell – free lysates, most predominantly used for protein synthesis from plant to animal cells. These have included the use of lysates from ubiquitous *Escherichia coli* [6, 18-20], rabbit reticulocytes, to wheat germ cells; all used for their specific properties. In the case of *E. coli*, the coupled transcription and translation machinery enables “one-pot” protein synthesis, but it is limited by the types of proteins synthesized such as post-translational modified proteins as well as mixed fraction proteins such as lipoproteins and proteins containing large portions of a carbohydrate moiety as found in

eukaryotic cells. While cell – free lysates from rabbit reticulocytes enable for full length and post-translational modified proteins, protein yields are less desirable due to the presence of nucleases and other endogenous RNAs that inhibit efficient translation [14]. In comparison to wheat germ based cell – free lysates, exotic RNAs such as double-stranded RNAs and proteins with heavy thiol moieties are translated with high efficiencies, but these cell – free lysates require 5' cap modifications to the mRNAs [15]. In examining the characteristics of each cell – free lysate in more detail under a variety of parameters, the function of these cell – free lysates can be further optimized.

Beyond utilization for protein synthesis, cell – free lysates are also the basis for input-output logic functions [5, 21]; several groups have explored the use of these components for diagnosis of disease and in detection of small molecules and environmental cues. Specifically, by combining the use of cell - free lysates to paper-based microfluidics, groups have used cell – free lysates as part of a detection device for the sensing of strain-specific pathogens like Ebola virus as well as toxins in the environment like arsenic [22-24]. However, due to the volume of samples needed to run paper-based cell – free diagnostics and the false positive detection rates, these devices may not be effective nor efficient in detecting pathogens and toxins in real-time. Limited volumes are especially pertinent when dealing with blood as an analyte. Others have improved the reliability and sensitivity of these devices using high-throughput microfluidics, but these also require the use of volumes > 100 μ L of analyte solutions [25, 26]. One possible answer to the volume problem is to reduce the reaction volume and take advantage of the nM sensitivity of these lysates through the encapsulation of cell – free lysates in engineered small vessels that are semi-permeable to the environment.

Here, we show a method combining the advantages of the aforementioned microfluidics techniques to detect and report the presence of *Pseudomonas* infection into a single platform—with an emphasis on portability, sensitivity, and durability of these cell – free systems in unfavorable biological and chemical environments. We demonstrate the successful utilization of co-localization of cell – free transcription and translation processes into a porous agarose microparticle for use as a biosensor and quantification tool (Figure 1, SI Figure 1).

Results and Discussion

By engineering a cell – free lysate system coupled with a *lasR*-based transcriptional activation mechanism, a model system for the detection of quorum sensing molecules can be utilized for prototyping of a biosensor. Specifically, several species such as *E. coli*, *Salmonella typhimurium*, *Vibrio harveyi*, as well as *Pseudomonas aeruginosa* utilize the *lasR* system for regulation of cell density, where endogenous LasR is induced by homoserine lactones (HSL) to activate the transcriptional activities for proteases and other enzymatic processes that inhibit cellular proliferation [27, 28]. The presence of HSL molecules enables LasR to form multimer assemblies such that LasR is unable to bind to the promoter regions of genes that encode for these proteases [29, 30]. Additionally, only through suppression of LasR are the genes responsible for virulence, cellular growth and development activated. In isolating the sensing component from the quorum sensing complex and coupling a reporter, a benign *lasR*-based biosensor having no virulent properties can be constructed for detection and reporting of *Pseudomonas* growth (Figure 1). Specifically, a *lasR*-based inducible promoter coupled to a GFP construct is utilized to fluoresce when a critical threshold of an acyl-HSL, specifically N 3-oxododecanoyl homoserine lactone (3OC12HSL), is present. Under *Pseudomonas aeruginosa* virulence, HSL causes the LasR protein to unbind from the promoter and allows expression of virulent genes. In this case, expression of a GFP reporter is activated and “virulent states” can be observed optically (Figure 1,2). Here, a *lasR*-based inducible transcription mechanism typically relied upon for regulation of virulence genes responsible for DNA replication, RNA transcription and translation, biofilm formation, and antibiotic resistance is co-opted for use in translation of a GFP reporter in the sensing and reporting of *Pseudomonas* infections.

In integrating this lasR-based mechanism into a delivery system that is permeable, size controlled and chemically inert, the reaction volumes required for efficient detection is decreased and sensitivity range is increased by being able to tune the effective concentrations of the components that make up the system unlike other groups [31] [20]. This delivery system is based on the use of hydrogel agarose microscale beads which we utilize to encapsulate the cell – free lysate and couple with transcription and translation (TXTL) processes (SI Figure 1). The size of the final microscale beads can be adjusted from diameters of 10 μm – 100 μm with minor adjustments to flow and pressure to the microfluidic processing and the porosity is an innate property of the cross-linking density of the agarose which can be controlled by agarose concentration [32] [33]. The resulting cell – free hydrogel device is a robust biosensor that can be delivered to both biologically and chemically hostile environments for controlled sensing and signaling of *Pseudomonas* infection.

The formation of the agarose beads encapsulating the TXTL LasR processes is performed through a controlled flow focusing microfluidic device using fluorinated oils and aqueous phase [34, 35] (SI Figure 1). The controlled flow of an aqueous component into an oil phase allows for the precise formation of aqueous droplets encapsulated by oil through phase separation (SI Figure 2). The low concentration of agarose utilized (1%) enable for achieving a molten phase at 45° C, a temperature that does not appear to degrade or denature the LasR protein based mechanism of detection. The 1:1 agarose:aqueous phase (consisting of the TXTL components and solvent) is contained in a microfluidic droplet and allowed to cool such that the agarose phase transitions from a molten phase to a solid phase incorporating the TXTL components in its porous structure (SI Figure 2). These TXTL extracts have been shown previously to be fully functional after lyophilization and reconstitution processes [31]. Accordingly, these agarose TXTL beads undergo further a lyophilization process to prevent diffusion of TXTL components from the bulk of the agarose bead to the surface; further enabling long term storage and utility of the TXTL components contained in the agarose beads.

By hydrating the lyophilized agarose TXTL beads, the lasR-based detection mechanism is activated and ready to signal the presence of any HSL in solution. This signal is itself roughly 30% more intense than the same lasR signaling mechanism performed in a bulk solution and can last even longer (Figures 2, 3) using the same volumes. By analyzing the rRNA in the beads compared to that in bulk solution, the amount of rRNA is dramatically lower in the functional agarose beads and the sensitivities are approximately 4 times higher in some cases (SI Figure 3). As reported in previous literature, the GFP signal is indeed an HSL induced and a function of the LasR protein concentration found in the TXTL reaction [36] [37]. This is also the case of the agarose TXTL beads where at approximately 3 μL of the stock lasR plasmid (100 nM lasR stock) used was found to provide for a stochastic signal of the GFP, indicating that at this concentration of LasR, there is a Poisson's distribution of binding with LasR and HSL, and subsequently translation of the GFP signal (SI Figure 4a). This distribution is also validated by fluorescence activated cell sorting (FACS) of the fluorescent beads which observes two distinct populations (approximately 10% are fluorescent of total number of beads measured) of fluorescent agarose TXTL beads in the same concentration range of 1 μM HSL (Figure 3a,b and SI Figure 5). Beyond this concentration of LasR utilized in the TXTL reaction, a shift of an oversupply of LasR binding is found. This is especially noteworthy since LasR binding to HSL should be highly dependent on competitive binding due to the multimeric binding of LasR to HSL, further indicating that no cooperativity exist in the LasR-HSL interaction. It may be indicative of an assembly mechanism with LasR such that a cooperative binding mechanism may occur whereby multiple LasR are bound to a single molecule of HSL [28] [38]. This would explain the shift in GFP production as well as LasR binding to HSL even in excess of LasR molecules (SI Figure 4a).

A caveat to utilizing a construct based on T7 RNA polymerase and linear plasmid system to reconstitute the lasR-based mechanism in TXTL is the innate degradation

mechanisms in *E. coli* that serve to prevent foreign genomic material as well as errors in transcripts from propagating into the cell cycle through the activity of endo- and exo- nucleases [39, 40]. In order to overcome these natural mechanisms inherent in *E. coli*-based TXTL extracts that degrade exogenous oligonucleotides, nuclease inhibitors are utilized. We observe that with the addition of GamS, a small molecule inhibitor of exonuclease activity inherent in these TXTL extracts [8, 20], the lasR mechanism is observed to possess increased signal sensitivity. The addition of a GamS component to the aqueous fraction during the formation of the agarose TXTL beads results in a 30% increase of signal observed immediately in the sensing and reporting of the presence of HSL using the lasR mechanism in comparison to the same population of agarose TXTL beads without GamS treatment (SI Figure 4b). And over a course of 12 hours, both the non-GamS and GamS treated agarose TXTL beads reach a plateau in signal. This indicates that exonuclease activity is time-dependent and activity is concentrated in the initial rounds of transcription and translation (SI Figure 4b). In essence, to thwart the activity of exonucleases in the absence of nuclease inhibitors like GamS, exogenous plasmids can be in excess such that the transcription and translation activities run longer than the exonuclease activity.

Contrary to standard concentrations utilized to evaluate the dose dependence of the lasR quorum sensing in bulk, the concentrations utilized in the agarose TXTL beads using similar fluorescence imaging are in the saturation range where the dose responses result in dose independent responses (Figure 3c). This indicates that the regime of the dose dependence is lower from the concentration of the lowest concentration range utilized here, 10 nM, implicating the quorum sensing of the lasR system in the form of agarose TXTL beads is on the order of pM sensitivity. In fact, by increasing the concentration 4 orders of magnitude higher to 10 μ M, to that observed in the bulk TXTL reactions, there is a further decrease in fluorescence indicating dose independent behavior (Figure 3c).

To evaluate the compatibility of this agarose TXTL bead platform for *Pseudomonas* detection *in vivo*, high spatial and temporal resolution obtained from 3D-structured illumination microscopy (3D-SIM) is utilized to track the spatial interactions of this system in the presence of live cells [41]. Traditionally, one difficulty to perform such observations is the ability to obtain enough depth of field to accurately obtain a representative cell population as well as high sensitivity to resolve and differentiate individual cells in the sample. This 3D-SIM method enables for the imaging of both the agarose TXTL bead as well as features found in single micron scale *Pseudomonas* cells (Figure 4). Specifically, a *Pseudomonas aeruginosa* strain (ATCC # BAA-1744) is initially incubated to obtain the mid-log phase of cell growth and is exposed to the agarose TXTL bead which results in the fluorescence of the bead. The media used for the mid-log phase of the cell cultures is also tested to determine whether the beads demonstrate fluorescence without cells. As shown in Figure 4, the *Pseudomonas* cell culture contains the autoinducer and triggers fluorescence in the beads. In previous plate-based experiments utilizing *Pseudomonas* cultures found in fecal tissue, the agarose TXTL beads were able to report induced signals (SI Figure 6). And the induced fluorescence demonstrates that the nM concentration of LasR produced from live cells is indeed within the thresholds of the agarose TXTL bead platform for rapid and detection of *Pseudomonas in vivo* as well.

Further modification of the agarose TXTL system to optimize detection of not only *Pseudomonas* infections, but also other quorum sensing based infections in general is shown here as feasible. As shown in SI Figure 7, the lasR quorum sensing is conserved within several bacterial groups and subsequently, the agarose TXTL bead platform would be effective in detecting the infections of other respective bacteria [42]. The binding of LasR to the respective DNA motifs can be analyzed through a DNA footprint analyses [43]. As shown in SI Figure 7b, the DNA motifs utilized by various bacteria are themselves conserved, while maintaining a high affinity for LasR. This indicates that bacteria have co-evolved to utilize the LasR transcriptional activities. More realistically, in cases of infection involving multiple bacteria, the agarose TXTL

bead system itself can be modified such that multiple quora sensing mechanisms representing a diversity of bacteria can be embedded such that the detection of multiple infections can be scaled-up.

Here we have demonstrated the ability to design a sensor-reporter pair integrated into agarose TXTL beads based on genetic circuits with a known input-output relationship, but it is also possible to leverage the high-throughput scalability of droplet-based microfluidics to identify gene circuits that detect novel input signals and optimize reaction conditions. As detailed in previous reports, libraries containing millions of unique gene combinations can be assembled in discrete agarose TXTL beads and assayed for reporter activity [44] [45]. Agarose TXTL beads containing sensitive and specific sensor-reporter circuits can be enriched by FACS-like sorting procedure and the DNA contents can be sequenced to identify the constituent genes [46]. Although this approach does not require foreknowledge of endogenous regulatory responses, the efficiency of engineering detectors may be improved by basing gene libraries to be screened on published transcriptomic data describing gene expression responses to specific signal inputs. We anticipate that these approaches will lead to the development of sensors for a broad range of molecular inputs such as bacterial stress signals and virulence factors which could provide important information related to mechanisms of antibiotic resistance and biofilm formation occurring in the analyte [47] [48] [49].

In this work, the utility of a cell – free agarose TXTL bead platform for rapid detection and sensing of *Pseudomonas* infections is shown. By having early detection and quick quantification of *Pseudomonas* specific infection, diagnosis and treatment to address the initial stages of pathogenesis can assist in limiting duration and severity of illness as well as excess use of antibiotic drugs. The agarose TXTL bead platform can also accommodate genetic reporter circuits that detect the presence of pathogens other than *Pseudomonas* as well as small molecules that carry additional information such as bacterial signals promoting virulence or antibiotic resistance. [47] [48] [49, 50]. As this platform is amenable to multiplexing of sensors, it will be possible to assay several parameters simultaneously for rapid assessment of pathogen prevalence and population state. As shown in the aforementioned figures, unlike other *in vivo* engineered detection systems of pathogens [37], this platform can be stored in dry and hostile environments indefinitely and deployed within minutes with very little hydration < 100 μ l. From the thorough understanding of the components of this integrated agarose TXTL bead platform, where each component can be further engineered and optimized, these mechanisms involved can be configured according to very specific applications (SI Figure 7c).

Methods and Materials

Cell – free lysate and TXTL extracts

Cell – free lysates are produced as described in Sun and coworkers [51] [8]. The energy buffer and lysates are combined into a single tube before the aforementioned encapsulation and lyophilization procedures. The LasR plasmid, GamS, and GFP constructs are gifts from the Laboratory of Richard M. Murray at Caltech.

Agarose encapsulation of TXTL

Using a microfluidic flow focusing device as seen in Abate et al. [35], an aqueous phase containing molten agarose (1%) along with the cell – free lysates, TXTL extracts, plasmids, and buffer are flowed into the device from one channel; the other channel fluorinated oil (3M 7500 HFE, St. Paul, MN 55144, USA) containing 2% surfactant, as performed by Holtze et al. [52], are flowed to make monodisperse agarose beads which are ~40 μ m in diameter.

Lyophilization and storage

The agarose TXTL beads are collected immediately after the microfluidic generation of drops and allowed to equilibrate at room temperature for 1 hour. Afterwards, the droplets are flash

frozen in liquid nitrogen and lyophilized overnight at a pressure of 30 mT (milliTorr) (Virtis Sentry 2.0, SP Scientific, Inc., Warminster, PA 18974, USA). The resulting lyophilized agarose beads are kept in dry storage and under controlled humidity.

Fluorescence Microscopy

In order to image the green fluorescence protein (GFP), an EVOS FL Auto Cell Imaging microscope (Invitrogen EVOS FL Microscope, Thermo Fisher Scientific, Inc., Waltham, MA 02454, USA) with automated stage controller was used to capture GFP as well as respective brightfield images.

RNA analyses

Agarose TXTL beads were rehydrated and activated. The activated beads were subjected to RNA extraction via Phenol:Chloroform treatment. The obtained RNA fraction was then prepared for analyses through the RNA 6000 Pico Chip Kit for activity and quality of the total RNA present in the samples. An Agilent 2100 Bioanalyzer (2100 Bioanalyzer, Agilent Technologies, Inc., Santa Clara, CA 95051, USA.) was used to quantify the RNA analyses.

Fluorescence plate reader

Plate reading measurements were conducted in 96-well flat, bottom well black plates (CellStar 96 Well Microplate, Greiner Bio-One GmbH, Kremsmuenster 4550, Austria) with a multimode plate reader (M200 multimode plate reader, Tecan Group AG, Maennedorf 8708, Switzerland) measurements from the top side. Overnight measurements were kept at constant 30°C temperatures during the reads and shaken for 1 second before reads.

Fluorescence Activated Cell Sorting (FACS)

After activating and collecting the agarose TXTL beads, the samples were subjected to double emulsification by way of encapsulation with flow focusing using a pluronic acid solution as the aqueous component such that the final double emulsified droplet size was ~50 µm in diameter. The double emulsified droplets were resuspended in water in a conical 5 mL test tube for mounting into the FACS (BD FACSAria, BD Biosciences, Inc., San Jose, CA 95131, USA). Data was acquired and saved in the BD format. Further data analyses and extraction was performed with the FlowJo 10.0 (FlowJo, FlowJo LLC, Ashland, OR 97520, USA) software suite.

3D-Structure Illumination Microscopy (3D-SIM) and Wide-Field Deconvolution Fluorescence Microscopy

Both conventional fluorescence microscopy and three dimensional-structured illumination microscopy (3D-SIM) images were acquired using the DeltaVision OMX SR V4 system with Blaze SIM module (GE Healthcare Life Sciences, Chicago, IL 60661, USA). The Deltavision OMX Blaze allows ultra-high speed illumination and acquisition, as described previously [41].

Samples were prepared by adding a 20 µl drop of bead/bacteria mixture on a standard microscope slide and sandwiching between a 22x22mm high precision coverslip (Bioscience Tools, San Diego, CA 92115 USA). Images were captured with a 50 ms exposure and 5% laser power on a PCO Edge scientific CMOS cameras dedicated to the 488 nm channel using an Olympus PlanApo N 60x 1.42 NA oil objective and standard excitation and emission filter sets (in nm, 488 EX/500–550 EM)(Olympus America, Center Valley, PA 18035 USA). 3D-SIM imaging was used to capture a small 4 or 6 µm thick sections of beads at a Z-spacing of every 125 nm. Unprocessed image stacks were composed of 15 images per z-section (five 72 degree phase-shifted images per angle at each of three interference pattern angles, +60, 0, and -60 degrees). Larger bead sections were acquired using the conventional widefield deconvolution imaging mode. 30 µm thick bead samples were captured using the same hardware as 3D-SIM

experiments but at 1 μm thick z-sections. Raw data from both 3D-SIM and widefield deconvolution modes were processed, deconvolved, and reconstructed in 3D using a constrained iterative algorithm (SoftWorX 4.0, GE Healthcare Life Sciences, Chicago, IL 60661, USA). Reconstructed images then exported and prepared for publication using ImageJ (NIH, Bethesda, MD 20892 USA) and Avizo 3D software (FEI, Hillsboro, OR 97124 USA) (Figure 4c and SI Movie 1).

Acknowledgements

J.S. would like to thank Drs. David Sukovich for technical assistance with the FACS measurements, Sean Poust, Joshua Cardiel, Iain Clark, John Haliburton, Tuan Tran, Colleen O’Laughlin, and Adam Abate for thorough discussions about this work. Dr. Andrew Jang (UCSF) is also acknowledged for technical assistance with Avizo rendering. The authors also thank the Center for Advanced Technologies (CAT), the Department of Biochemistry and Biophysics, and the DeRisi Laboratory at UCSF for access to imaging and characterization platforms. The laboratory of Richard M. Murray and Ms. Claire Hayes of Caltech are acknowledged for their reagents and cell – free expertise. Cell-free buffers and plasmids are donated from Dr. Zachary Sun of SynvivoBio, Inc. Funding for this work was provided through the Defense Advanced Research Projects Agency (DARPA) under the Living Foundries Program (HR0011-12-C-0065).

Figure Legend

Figure 1. Properties of the lasR-based cell – free method in bulk and in agarose bead forms (A.) A schematic of the interactions between homoserine lactones and LasR proteins in relation to lasR regulation of transcription (B.) A GFP reporter system demonstrates the bulk regulation by lasR in transcription (C.) A crystal structure of the LasR-HSL bounded interaction [courtesy of PDB: 4Y90] (D.) A schematic demonstrating the use of the lasR-based mechanism in agarose TXTL beads.

Figure 2. Agarose TXTL bead based sensing and quantification using the lasR-mechanism (A.) The signal intensity differences observed between agarose bead versus bulk sensing (B.) Brightfield and Fluorescence images of the agarose TXTL beads (C.) Various concentrations of HSL (from 100 μM stock) added to the agarose beads to demonstrate HSL sensitivity in the lasR-based system (i.) 0 μl (ii.) 1 μl (iii.) 3 μl (iv.) 5 μl

Figure 3. Quantifying the characteristics of the agarose TXTL bead *in vitro* (A.) Fluorescence Activated Cell Sorting of the agarose TXTL bead sensing system with Cy5 as a background marker (B.) By quantifying the GFP signal, we find that approximately 10% of the total number of beads measured (C.) Dose independent behavior indicates the sensitivity of the agarose TXTL bead is closer to the nM than the μM concentrations of HSL. Also observed in are the effects of these doses over time which confirms stability of the sensor.

Figure 4. Imaging the sensing and reporting activities of agarose TXTL beads in cell cultures of (A.) *Pseudomonas aeruginosa* (B.) *Escherichia coli* control (C.) 3D Reconstructed image of individual *Pseudomonas* cells and agarose TXTL bead

Supplementary Information (SI) Figure Legend

SI Figure 1. A schematic demonstrating the components of the lasR-based agarose TXTL bead formation and processing for *Pseudomonas* sensing and reporting

SI Figure 2. Interferometric imaging of the emulsions containing agarose TXTL beads (a.) Bright field imaging (b.) Tomographic reconstruction of the respective TXTL beads found in (a.) From

the refractive differences of the emulsions containing agarose beads, the various colors indicate different phases, the utilized components from the oil-surfactant outer layer of the emulsion (green) to the agarose beads themselves (white).

SI Figure 3. Total RNA analyses of bulk and agarose TXTL bead using the same lasR-based sensing and reporting mechanism with different

SI Figure 4. Stabilization of the lasR-based GFP signal (A.) By varying the lasR linear plasmid concentration, the GFP signal can be modulated (B.) The effect of the GFP signal following the addition of GamS to protect the linear plasmid from nucleases, in comparison to a non-GamS sample, can be observed to improve the GFP signal instantaneously.

SI Figure 5. FACS related sorting of the fractions of the GFP positive signals with 1

SI Figure 6. Plot of GFP signal intensity of the lasR-based agarose TXTL bead biosensor system in a real-world biological environment such as fecal analyte observed via plate-based fluorescence assay

SI Figure 7. Sequence analyses of LasR and LasR-like homologs (A.) At the protein sequence level to demonstrate relationships to other transcriptional activators (B.) Of the interacting DNA binding footprints of LasR-like proteins found in various species (C.) A schematic demonstrating the possible concept of adapting agarose TXTL beads for diverse applications

SI Movie 1. 3D SIM imaging of the agarose TXTL beads in culture with *Pseudomonas* cells. An animation of the 3D reconstruction of *Pseudomonas aeruginosa* and activated agarose TXTL beads

References

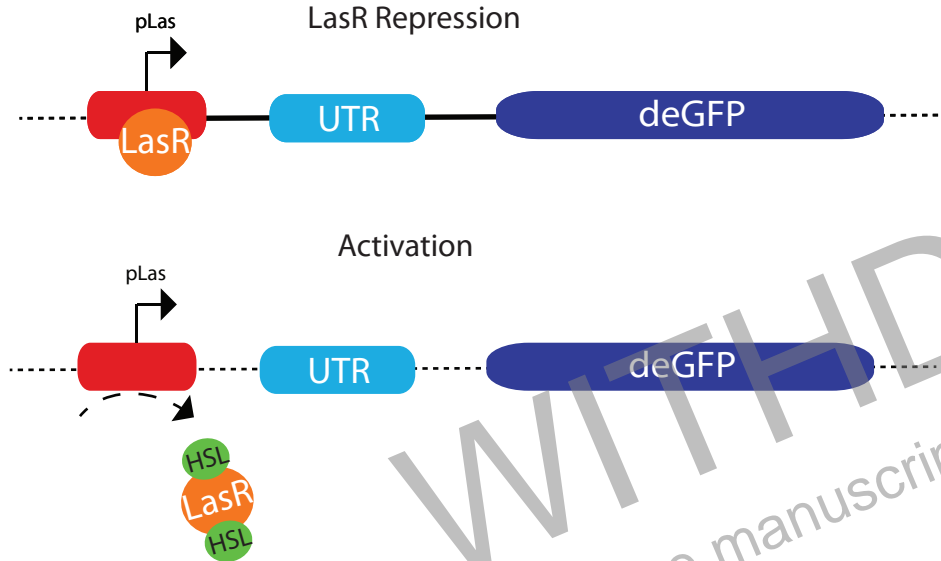
1. DiCarlo, J., et al., *Safeguarding CRISPR-Cas9 gene drives in yeast*. Nat Biotech, 2015. **33**(1250-1257): p. 1-6.
2. Knight, S., et al., *Dynamics of CRISPR-Cas9 genome interrogation in living cells*. Science, 2015. **350**(6262): p. 823-826.
3. Kotula, J., et al., *Programmable bacteria detect and record an environmental signal in the mammalian gut*. PNAS, 2014. **111**(13): p. 4838-4843.
4. Isaacs, F., et al., *Precise Manipulation of Chromosomes in Vivo Enables Genome-Wide Code Replacement*. Science, 2011. **333**: p. 348-353.
5. Moon, T., et al., *Genetic programs constructed from layered logic gates in single cells*. Nature, 2012. **491**(7423): p. 249-253.
6. Noireaux, V., R. Bar-Ziv, and A. Libchaber, *Principles of cell-free genetic circuit assembly*. PNAS, 2003. **100**(22): p. 12672-12677.
7. Noireaux, V. and A. Libchaber, *A vesicle bioreactor as a step toward an artificial cell assembly*. PNAS, 2004. **101**(51): p. 17669-17674.
8. Sun, Z., et al., *Linear DNA for Rapid Prototyping of Synthetic Biological Circuits in an Escherichia coli Based TX-TL Cell-Free System*. ACS Syn Biol, 2014. **3**: p. 387-397.
9. Koerber, J., M. Hornsby, and J. Wells, *An Improved Single-Chain Fab Platform for Efficient Display and Recombinant Expression*. J. Mol. Biol., 2015. **427**: p. 576-586.
10. Bar-Even, A. and D. Tawfik, *Engineering specialized metabolic pathways-is there a room for enzyme improvements*. Curr Opin Biotechnol, 2013. **24**: p. 310-319.

11. Jewett, M., et al., *An integrated cell-free metabolic platform for protein production and synthetic biology*. Mol Sys Biol, 2008. **4**(220): p. 1-10.
12. Harris, D. and M. Jewett, *Cell-free biology: exploiting the interface between synthetic biology and synthetic chemistry*. Curr Opin Biotechnol, 2012. **23**(5): p. 672-678.
13. Albayrak, C. and J. Swartz, *Cell-free co-production of an orthogonal transfer RNA activates efficient site-specific non-natural amino acid incorporation*. Nuc. Acids Res., 2013. **41**(11): p. 5949-5963.
14. Endo, Y. and T. Sawasaki, *Cell-free expression systems for eukaryotic protein production*. Curr Opin Biotechnol, 2006. **17**(4): p. 373-380.
15. Goshima, N., et al., *Human protein factory for converting the transcriptome into an in vitro-expressed proteome*. Nat Methods, 2008. **5**(12): p. 1011-1017.
16. Crick, F., *Central Dogma of Molecular Biology*. Nature, 1970. **227**: p. 561-563.
17. Alberts, B., et al., *Molecular Biology of the Cell*. 6th ed. Molecular Biology of the Cell. 2014: Garland Science. 1464.
18. Shrestha, P., T. Holland, and B. Bundy, *Streamlined extract preparation for Escherichia coli-based cell-free protein synthesis by sonication or bead vortex mixing*. BioTechniques, 2012. **53**: p. 163-174.
19. Yang, W., et al., *Simplifying and Streamlining Escherichia coli-Based Cell-Free Protein Synthesis*. Biotechnol Prog., 2012. **28**(2): p. 413-420.
20. Kwon, Y. and M. Jewett, *High-throughput preparation methods of crude extract for robust cell-free protein synthesis*. Sci Rep, 2015. **5**(8663): p. 1-8.
21. Lentini, R., et al., *Fluorescent Proteins and in Vitro Genetic Organization for Cell-Free Synthetic Biology*. ACS Syn Biol, 2013. **2**: p. 482-489.
22. Pollock, N., et al., *A Paper-Based Multiplexed Transaminase Test for Low-Cost, Point-of-Care Liver Function Testing*. Science Transl. Med., 2012. **4**(152): p. 1-10.
23. Nath, P., R. Arun, and N. Chanda, *A paper based microfluidic device for the detection of arsenic using a gold nanosensor*. RSC Advances, 2014. **4**.
24. Pardee, K., et al., *Paper-Based Synthetic Gene Networks*. Cell, 2014. **159**: p. 940-954.
25. Streets, A., et al., *Microfluidic single-cell whole-transcriptome sequencing*. PNAS, 2014. **111**(19): p. 7048-7053.
26. Niederholtmeyer, H., et al., *Rapid cell-free forward engineering of novel genetic ring oscillators*. eLIFE, 2015. **10.7554**(eLife.09771): p. 1-21.
27. Ng, W. and B. Bassler, *Bacterial Quorum-Sensing Network Architectures*. Annu. Rev. Genet., 2009. **43**: p. 197-222.
28. Waters, C. and B. Bassler, *Quorum Sensing: Cell-to-Cell Communications in Bacteria*. Annu. Rev. Cell Dev. Biol., 2005. **21**: p. 319-346.
29. Gambello, M., S. Kaye, and B. Iglewski, *LasR of Pseudomonas aeruginosa Is a Transcriptional Activator of the Alkaline Protease Gene (apr) and an Enhancer of Exotoxin A Expression*. Infection and Immunity, 1993. **61**(4): p. 1180-1184.
30. Thaden, J., S. Lory, and T. Gardner, *Quorum-Sensing Regulation of a Copper Toxicity System in Pseudomonas aeruginosa*. J Bacter, 2010. **192**(10): p. 2557-2568.
31. Didovyk, A., et al., *Rapid and Scalable Preparation of Bacterial Lysates for Cell-Free Gene Expression*. ACS Syn Biol, 2017. **6**: p. 2198-2208.
32. Forget, A., et al., *Mechanically Tailored Agarose Hydrogels through Molecular Alloying with Beta Sheet Polysaccharides*. Mol Rapid Comm, 2014. **36**(2): p. 196-203.
33. Jagers, R. and S. Bon, *Communication between hydrogel beads via chemical signalling*. J Mater Chem B, 2017. **5**: p. 8681-8685.

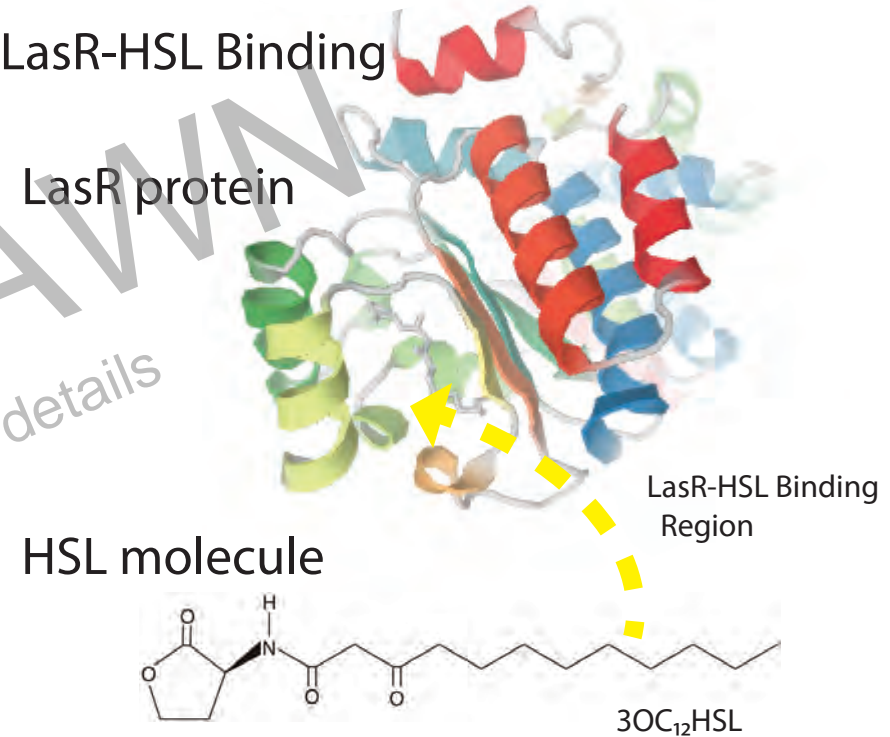
34. Agresti, J., et al., *Ultrahigh-throughput screening in drop-based microfluidics for directed evolution*. PNAS, 2009. **107**(9): p. 4004-4009.
35. Abate, A., et al., *High-throughput injection with microfluidics using picoinjectors*. PNAS, 2010. **107**(45): p. 19163-19166.
36. Chappell, J., K. Jensen, and P. Freemont, *Validation of an entirely in vitro approach for rapid prototyping of DNA regulatory elements for synthetic biology*. Nuc. Acids Res., 2013. **41**(5): p. 3471-3481.
37. Wen, K., et al., *A Cell-Free Biosensor for Detecting Quorum Sensing Molecules in P. aeruginosa-Infected Respiratory Samples*. ACS Syn Biol, 2017. **6**: p. 2293-2301.
38. Kiratisin, P., K. Tucker, and L. Passador, *LasR, a Transcriptional Activator of Pseudomonas aeruginosa Virulence Genes, Functions as a Multimer*. J Bacter, 2002. **184**(17): p. 4912-4919.
39. Eder, P., et al., *Substrate Specificity and Kinetics of Degradation of Antisense Oligonucleotides by a 3' Exonuclease in Plasma*. Antisense Res and Dev, 1991. **1**: p. 141-151.
40. Kerins, S., R. Collins, and T. McCarthy, *Characterization of an Endonuclease IV 3'-5' Exonuclease Activity*. J Biol Chem, 2003. **278**(5): p. 3048-3054.
41. Strauss, M., et al., *3D-SIM Super Resolution Microscopy Reveals a Bead-like Arrangement for FtsZ and the Division Machinery: Implications for Triggering Cytokinesis*. Plos Biol, 2012. **10**(9): p. 1-17.
42. Marchler-Bauer, A., et al., *CDD: NCBI's conserved domain database*. Nuc. Acids Res., 2015. **43**: p. 222-226.
43. Contreras-Moreira, B., *3D-footprint: a database for the structural analysis of protein-DNA complexes*. Nuc. Acids Res., 2010. **38**: p. 91-97.
44. Fallah-Araghi, A., et al., *A completely in vitro ultrahigh-throughput droplet-based microfluidic screening system for protein engineering and directed evolution*. Lab Chip, 2012. **12**: p. 882-891.
45. Hori, Y., et al., *Cell-free extract based optimization of biomolecular circuits with droplet microfluidics*. Lab Chip, 2017. **17**: p. 3037-3042.
46. Eastburn, D., A. Sciambi, and A. Abate, *Identification and genetic analysis of cancer cells with PCR-activated cell sorting*. Nuc. Acids Res., 2014. **42**(16): p. 1-10.
47. Gooderham, W. and R. Hancock, *Regulation of virulence and antibiotic resistance by two-component regulatory systems in Pseudomonas aeruginosa*. FEMS Microbiol Rev, 2008. **33**: p. 279-294.
48. Wagner, V., R. Gillis, and B. Iglewski, *Transcriptome analysis of quorum-sensing regulation and virulence factor expression in Pseudomonas aeruginosa*. Vaccine, 2004. **22**(S1): p. 15-20.
49. LeRoux, M., et al., *Kin cell lysis is a danger signal that activates antibacterial pathways of Pseudomonas aeruginosa*. eLIFE, 2015. **4**(e05701): p. 1-25.
50. Stanton, B., et al., *Genomic Mining of Prokaryotic Repressors for Orthogonal Logic Gates*. Nat Chem Biol, 2014. **10**(2): p. 99-105.
51. Sun, Z., et al., *Protocols for Implementing an Escherichia coli Based TXTL Cell-Free Expression System for Synthetic Biology*. JoVE, 2013. **e50762**(79): p. 1-14.
52. Holtze, C., et al., *Biocompatible surfactants for water-in-fluorocarbon emulsions*. Lab Chip, 2008. **8**(10): p. 1632-1639.

Figure 1.

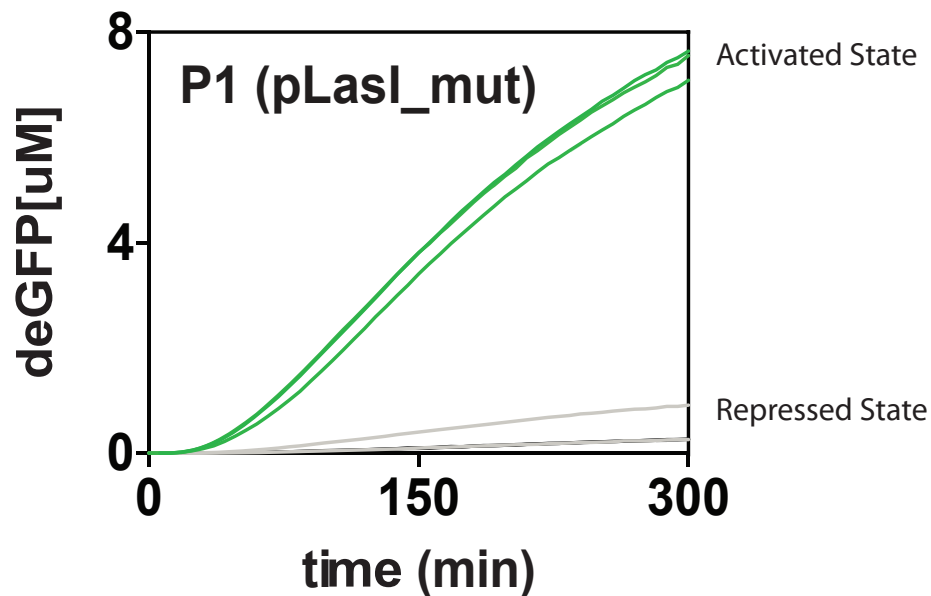
A. LasR-GFP Fusion construct



B. LasR-HSL Binding



C. GFP Expression in solution



D. Schematic of encapsulated TXTL reaction

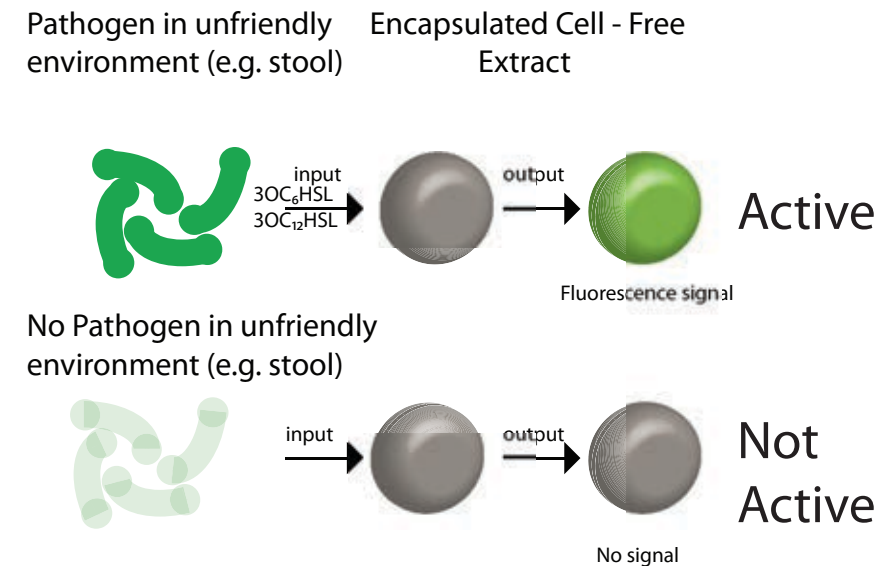
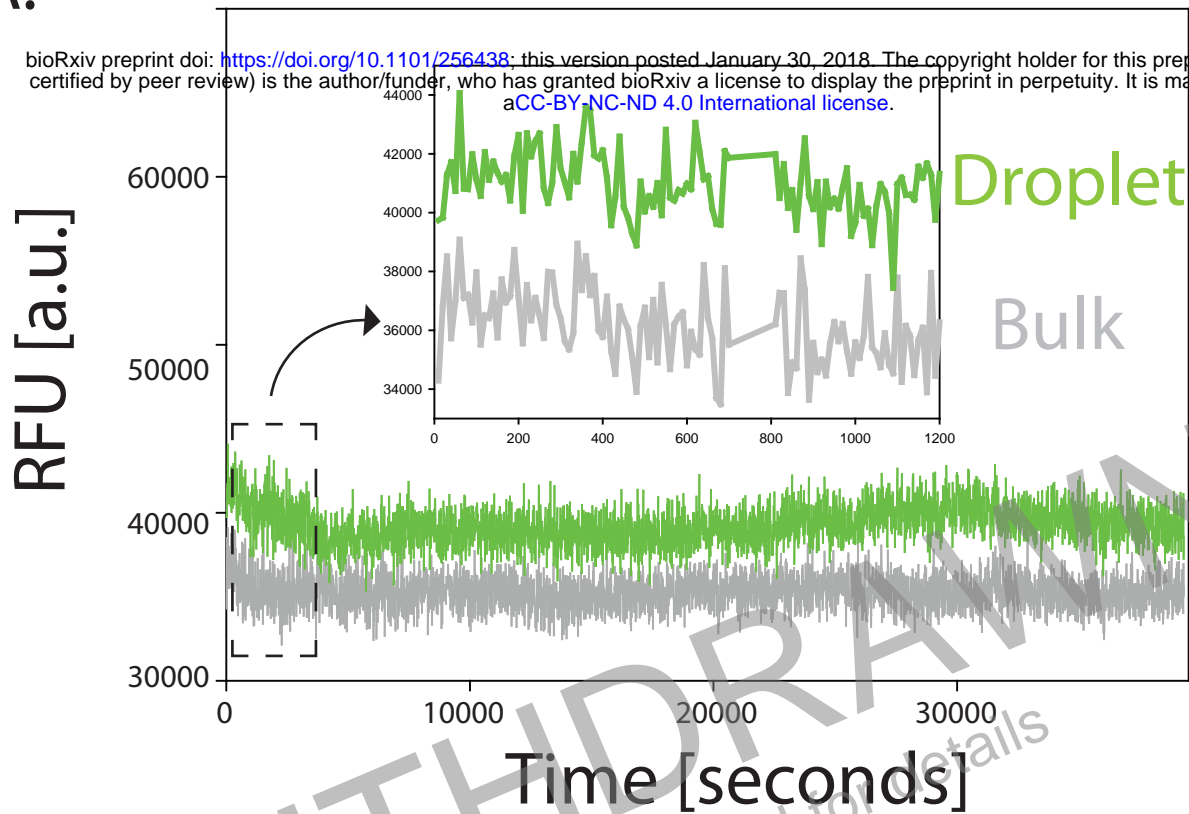


Figure 2.

A.



B. Brightfield Fluorescence

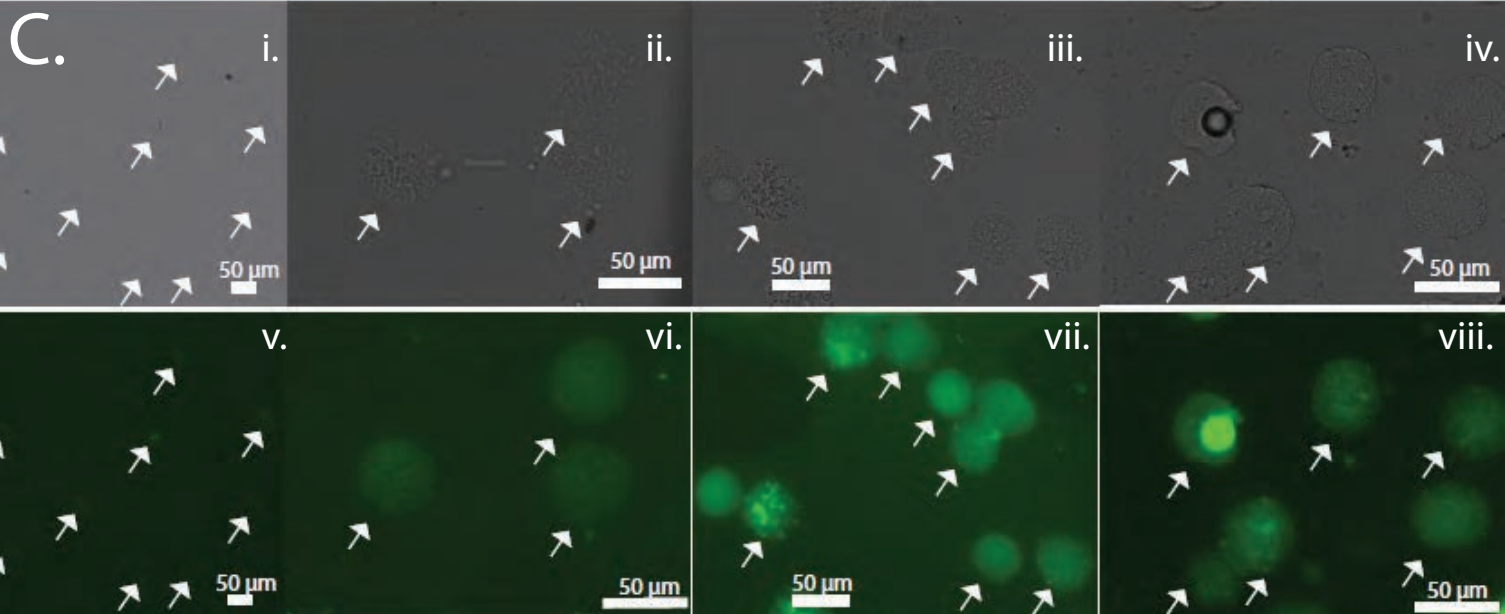
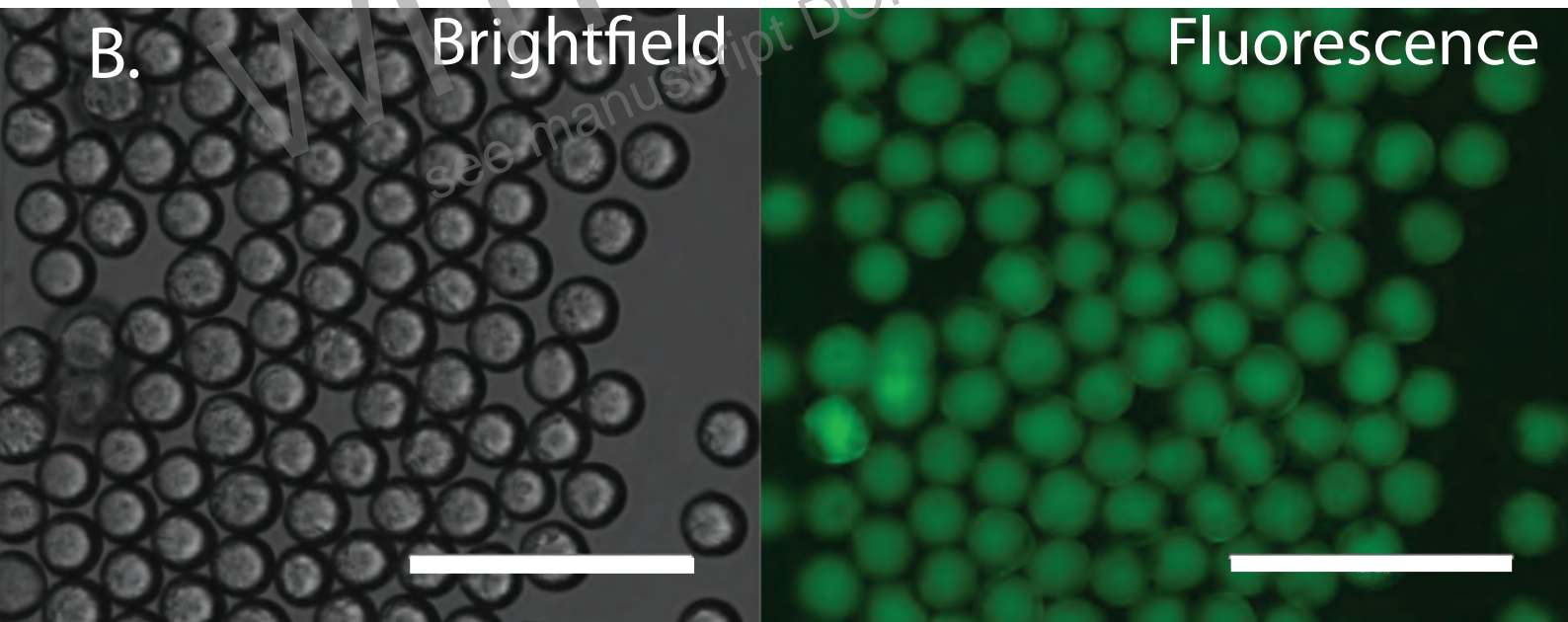


Figure 3

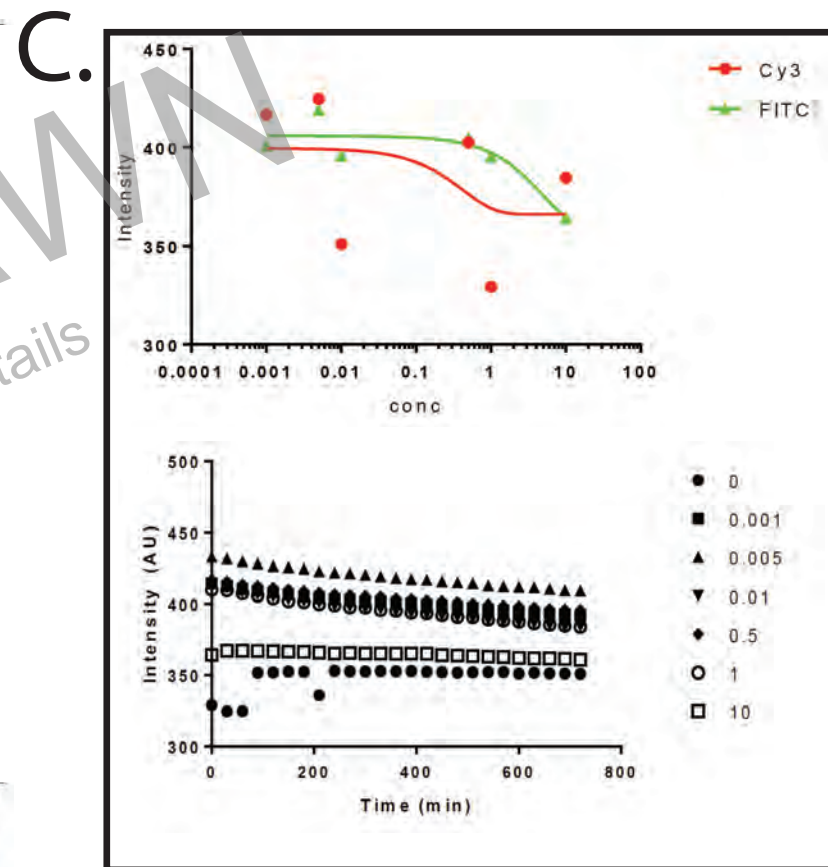
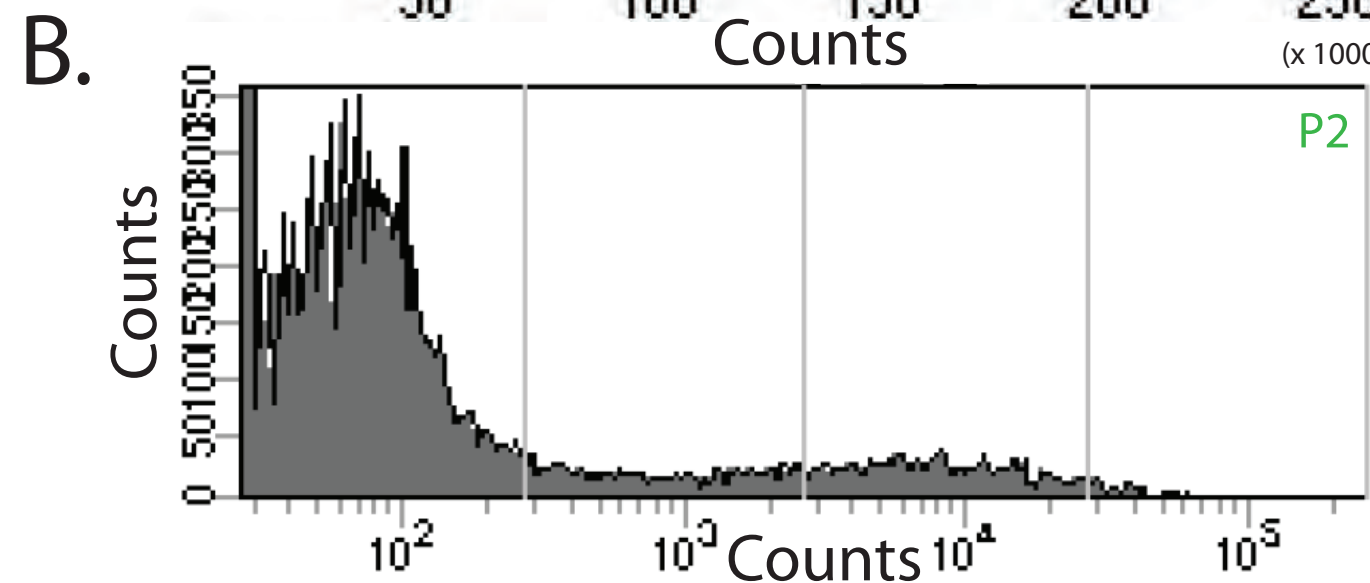
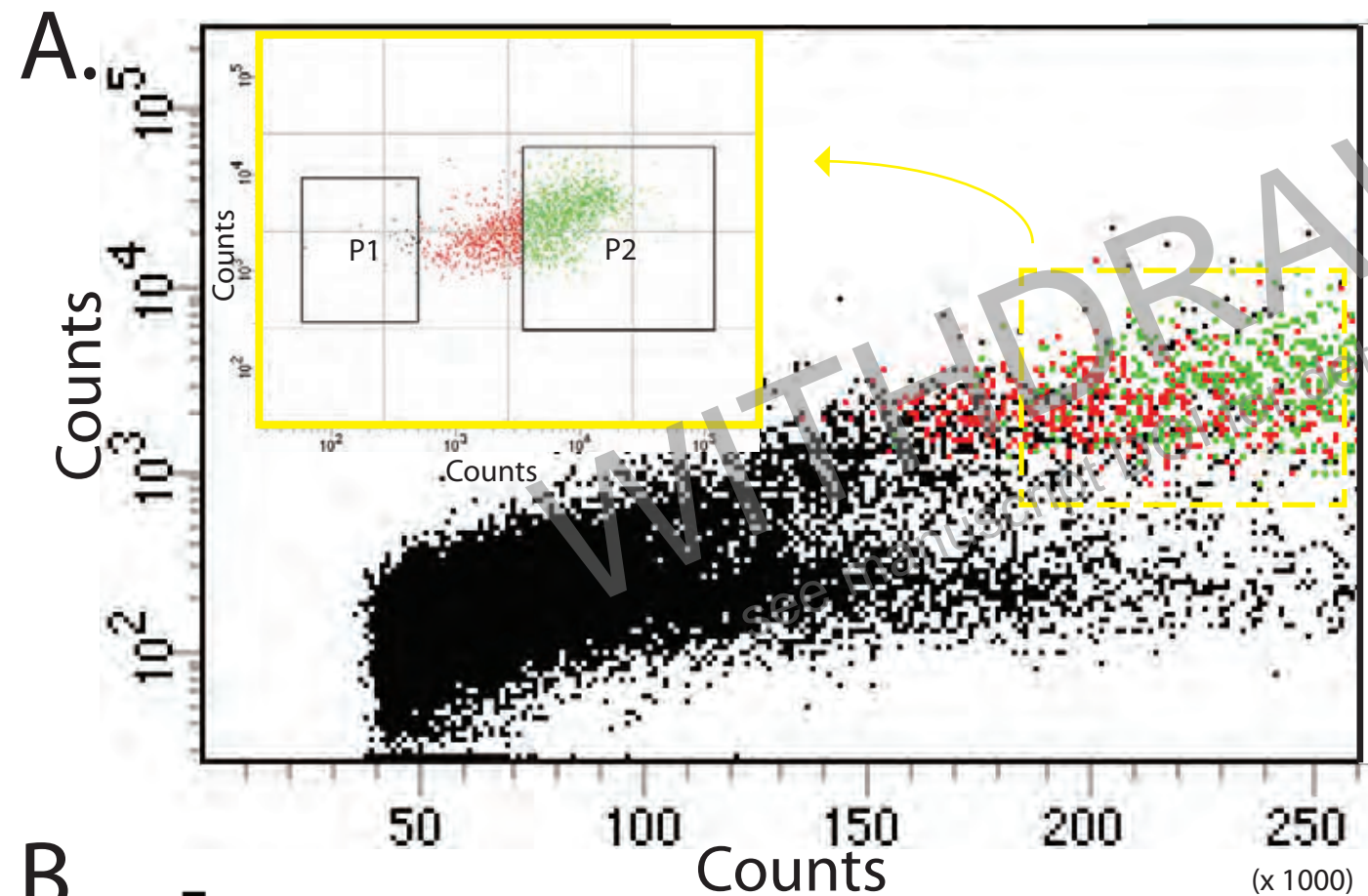


Figure 4.

bioRxiv preprint doi: <https://doi.org/10.1101/256438>; this version posted January 30, 2018. The copyright holder for this preprint (which was not certified by peer review) is the author/funder, who has granted bioRxiv a license to display the preprint in perpetuity. It is made available under aCC-BY-NC-ND 4.0 International license.

A. *Pseudomonas*

B. *E. coli*

Agarose TXTL Bead

C. 3D Image Reconstruction

Agarose TXTL Bead

Pseudomonas cells

